Cardioprotective effect of alphaB crystallin protein transduction and its action mechanism

Seungwon Yang

The Graduate School

Yonsei University

Graduate Program in Science for Aging

Molecular Cell Biology

Cardioprotective effect of alphaB-crystallin protein transduction and its action mechanism

A Master's Thesis Submitted to the Department of Graduate Program in Science For Aging and the Graduate School of Yonsei University in partial fulfillment of the requirements for the degree of Master in Science for Aging

Seungwon Yang

July 2008

This certifies that the masters thesis of

Seungwon Yang is approved.

_____

Thesis Supervisor: Yangsoo Jang

_____

Thesis Committee Member: Seok-Min Kang

_____

Thesis Committee Member: Ji Hyung Chung

The Graduate School

Yonsei University

July 2008

감사의 글

이 곳 노화과학 대학원에서 석사 학위를 시작한 게 엊그제 같은데 어느덧 졸업을 맞이 하게 되었습니다. 무엇보다도 이 곳에서 많은 배움을 얻고, 사고를 좀 더 넓힐 수 있는 기회를 가졌던 거 같아 뿌듯하고 한편으로는 많이 아쉽기도 합니다. 생각해 보면 실험실 생활 동안 저에게 도움을 주셨던 분들이 너무나 많습니다.

언제나 폭 넓은 격려를 아끼지 않으시는 장양수 교수님, 탁월한 관점으로 논문을 분석하시던 강석민 교수님, 언제나 저와 같이 실험 문제 해결을 위한 고민을 해 주시며 뛰어난 아이디어와 냉철한 분석을 통해 저에게 큰 힘이 되어 주셨던 정지형 교수님께 우선적으로 깊은 감사를 드립니다.

석사 과정 동안 제가 몸 담고 일했던 우리 노화기전 연구실에 식구들에서 또한 큰 감사를 드립니다. 우선, 우리 실험실에 Postdoc 으로 계시면서, 실질적으로 전반적인 실험들을 컨트롤 하시고, 이 논문을 준비함에 있어 다방면에서 크나큰 도움을 주신 이경혜 박사님, 동물 실험의 대가로 불리우며 언제나 따뜻하게 대해 주시고 많은 먹거리를 제공해 주시는 김일권 선생님, 석사 초반 실험의 즐거움을 알게 해준 임은경 선생님, 깔끔한 실험 테크닉을 알려주시고, 실험 방법적인 면에서 많은 해결책을 제시해 주시던 신혜진 선생님, 항상 앞을 향해 전진 하시는 권준혜 박사님, 얼마 전

공주님을 출산하신 착한 신보희 선생님, 말수는 적지만 따뜻한 마음을 가지고 계신 조봉준 선생님, 언제나 편한 대화 상대가 되어준 장강원씨, 실험실 동기이자 석사 2년 동안 여러 모로 다양한 도움을 주면서 웃음을 잃지 않는 착한 동생 김수혁, 항상 바쁘게 뛰어다니면서 실험실의 궂은 일을 앞장서서 하는 진태원씨, 고민이 생겼을 때 항상 해결책을 제시해 주시며 Tough Cho 를 강조하는 조현희형, 언제나 질문이 많고 실험적 열의가 강하신 유기준 선생님 등 우리 노화기전 연구실 식구들에게 감사하는 마음을 간직 하고, 다들 뜻한 바를 이룰 수 있기를 바라겠습니다.

2년 동안 같이 수업 들으면서 여러모로 도움을 주신 우리 노화과학 대학원 식구들…

모든 일에 최선을 다하시는 이기호 선생님, 언제나 친철하게 대해 주시는 이세영선생님,코멘트가 인상적인 하창영선생님, 주위 사람들을 즐겁게 해 주시는 오세연 선생님, 맡은 일에 책임이 강하신 김범식 선생님, 언제나 털털하고 유쾌함을 유지하는 여현양, 모든 일에 최선을 다해 임하는 곽정현씨, 내 석사과정 동기이자 많은 도움을 주었던, 친한 친구 같은 동생들 강미란, 김소의, 많이 친해 지지는 못했지만 착한 노화과학 후배들 한지혜,오지희,강주희씨… 다들 그 동안 감사했습니다.

현재 각기 다른 곳에서 각자에 실험에 매진하고 있고, 실험적 discussion 에 많은 도움을 준 우석이형, 재준이형, 현중형에게도 감사를 전합니다. 그리고 나를 잘 따라주고, 좋은 해결책들을 제시해 주며, 언제나

힘이 되어주는 미진이에게 또한 감사를 전합니다.

무엇보다도 제가 여기까지 올 수 있게 언제나 내편에 서서 응원을 해 주시며, 지원을 아끼지 않으셨던, 우리 가족 아버지, 어머니, 형, 형수님께 깊은 감사를 드리며, 이만 감사의 글을 접으려 합니다. 이곳에 다 기재 하지 못했지만 저를 아껴 주시고 여러 모로 도움을 주시고 계신 분들이 너무나 많이 계시고, 그 분들께 항상 감사히 생각 하고 있습니다. 이 모든 분들에게 이 논문을 바칩니다.

TABLE OF CONTENTS

ABSTRACT ····· 1

I. INTRODUCTION ····· 4

II. MATERIALS AND METHODS ····· 9

1. Molecular cloning of human αB crystallin ····· 9

2. Expression and purification of αB crystallin fusion proteins ····· 10

3. Animal cell culture ····· 11

4. Transduction of TAT-αB crystallin fusion protein into cells ····· 11

5. Immunoblot analysis ····· 12

6. Immunoprecipitation ····· 13

7. Immunocytochemistry ····· 14

8. Measurement of caspase-3 activity ····· 14

9. Matrix metalloproteinase cleavage assay ····· 15

10. Preparation of detergent-insoluble fraction ····· 15

11. Mitochondrial and cytoplasmic cell fractionation ····· 16

III. RESULTS ····· 17

1. Construction and purification of αB crystallin fusion protein ····· 17

2. Transduction of TAT-αB crystallin into H9c2 cell ····· 19

3. Protective effect of TAT-αB crystallin in H9c2 cell ····· 21

4. Antiapoptotic effect of TAT-αB crystallin ····· 24

5. The cleavage of the transduced TAT-αB crystallin in H9c2 cell ···· 27

6. Different cleavage patterns of TAT-αB crystallin in soluble and insoluble fraction of cells ····· 29

7. Cleavages of TAT-αB crystallin by matrix metalloproteinase-1 ···· 32

8. Cleavage of recombinant αB crystallin and TAT-αB crystallin by matrix metalloproteinase-1····· 34

9. Cleavages patterns of TAT-αB crystallin by various matrix metalloproteinases ····· 36

10. Cleavage site within TAT-αB crystallin by matrix metalloproteinases ····· 38

11. Time-dependent cleavage of TAT-αB crystallin by matrix metalloproteinases ····· 40

12. Effect of matrix metalloproteinases inhibitors on the cleavage of TAT-αBcrystallin ····· 42

13. Suppression of cleavage of TAT-αB crystallin by the inhibitors of MAP kinases and matrix metalloproteinases ····· 44

14. Activation of Jun N-terminal kinase and matrix metalloproteinase-3

by TAT-αB crystallin transduction in cells ····· 46

IV. DISCUSSION ····· 48

V. REFERENCES ····· 54

ABSTRACT (In Korean) ····· 65

LIST OF FIGURES

Fig. 1. Construction and purification of αB crystallin fusion protein ··18

Fig. 2. An analysis of intracellular TAT-αB crystallin fusion proteins in H9c2 cells ·····20·····

Fig. 3. Transduction of TAT-αB crystallin and its protective effect against staurosporine-induced cell death ·····23·····

Fig. 4. TAT-αB crystallin prevents staurosporine-induced cytochrome C release and caspase-3 activation ·····26····

Fig. 5. Cleavage of transduced TAT-αB crystallin in H9c2 cell ·····28··

Fig. 6. Concentration- and time-dependent transduction of TAT-αB crystallin and different cleavage patterns between soluble and insoluble fraction·····31·····

Fig. 7. Specific cleavage of TAT-αB crystallin by MMP-1·····33··

Fig. 8. Cleavage of recombinant αB crystallin and TAT-αB crystalline by MMP-1 ·····35·····

Fig. 9. Cleavage patterns of TAT-αB crystallin by MMPs ·····37··

Fig. 10. An analysis of cleavage site within TAT-αB crystallin by MMPs ·····39·····

Fig. 11. Time-dependent cleavage of TAT-αB crystallin by MMPs·····41

Fig. 12. Effect of solubility of TAT-αB crystallin by MMP inhibitor ·····43

Fig. 13. Effect of MAP kinase inhibitors on the cleavage of TAT-αB crystallin ·····45

Fig. 14. TAT-αB crystallin transduction induces MMP-3 and JNK activation in cells ·····47

ABSTRACT

Cardioprotective effect of alphaB-crystallin protein transduction and its action mechanism

Seungwon Yang

Graduate Program in Science for Aging

The Graduate School, Yonsei University

(Directed by Professor Yangsoo Jang)

Small heat shock proteins (sHSPs) provide defense mechanism against stresses as heat shock, oxidative stress and hyperosmotic stress. One such protein is alpha B crystallin (αB crystallin) which is present at considerable levels than other sHSP in the heart, skeletal muscle, and kidney and plays a

critical role in repression of the aggregation of denatured proteins. Recent studies have been established that the overexpression of αB crystallin highly improves antiapoptotic effect against staurosporine-induced apoptosis through repression of cytochrome C release, interaction with members of the Bcl-2 family and inhibition of caspase-3 activity. In this study, using protein delivery system, we studied the potential cardiac protective effect of αB crystallin as a therapeutic protein in rat cardiac myoblast H9c2 cells and its cleavage and degradation mechanism by matrix metalloproteinases (MMPs) during TAT-αB crystallin transduction. The results showed that TAT-αB crystallin was effectively transduced across the plasma membrane and located in not only cytoplasm but also nucleus, and TAT-αB crystallin had strong antiapoptotic effect in staurosporine-induced apoptosis such as the repression of cytochrome C release, binding to Bax and inhibition of caspase-3 activity. And we showed that TAT-αB crystallin colocalizes with cytoskeleton components such as β-tubulin during staurosporine-induced cell death. It probably acts as a protective effector of the cytoskeleton and influences recovery and stability of cytoskeleton. Moreover, we found that TAT-αB crystallin were cleaved during transduction and also found that recombinant MMP-1,-3,-7,-8,-9 proteins had endopeptidase activity at TAT-αB crystallin *in vitro*. The transduction of TAT-αB crystallin induced MMP-3 activation and

Jun N-terminal kinase (JNK) phosphorylation. In deed, the cleavage of TAT-αB crystallin was attenuated by inhibitors of MMP-3 and JNK in H9c2 cell. TAT-αB crystallin had strong antiapoptotic effect against staurosporine-induced cell death such as the repressing cytochrome C release, inhibiting caspase-3 activity and binding with Bax.

Key Words: Alpha B crystallin, Protein transduction domain, Matrix metalloprotease, Small heat shock protein, Apoptosis

Cardioprotective effect of alphaB-crystallin protein transduction and its action mechanism

Seungwon Yang

Graduate Program in Science for Aging

The Graduate School, Yonsei University

(Directed by Professor Yangsoo Jang)

I. INTRODUCTION

Heat shock proteins (HSP) are a group of proteins whose expression is increased when the cells are exposed to elevated temperatures or other stress. Small heat shock proteins are a family of proteins with molecular weights of

generally less than 30 kDa. The sHSPs play a critical role in repression of the aggregation of denatured proteins.[1] The mechanism is an energy-independent process and organismal defense during physiological stress where they protect proteins from irreversible aggregation until suitable conditions pertain for renewed cell activity, at which time protein release and refolding are mediated by ATP-dependent chaperones such as HSP70.[4,9,24]

Another important role of small HSPs is their antiapoptotic function during differentiation and development, in particular by inhibiting the processing and activation of caspases and cytochrome c release.[1,3] Therefore, they highly affect to protect cells against stress factors such as heat shock, oxidative stress and hyperosmotic stress.[4,5] One of these small HSPs is alpha B crystallin (αB crystallin) which is present at considerable levels better than other sHSP in the heart, skeletal muscle, and kidney and it can be induced highly by heat and other stresses.[6]

The expression of crystallin changes during development. For example, in postnatal rat lenses, only oligomeric heat shock factor-heat shock element complexes are detectable, whereas in the fetal lens only monomeric complexes are found. This suggests that transcription of αB crystallin gene is developmentally regulated,[28] and αB crystallin is associated with diseases related to aggregation. It was reported that the R120G missense mutation in

αB-crystallin cause a desmin-related cardiomyopathy.[29] Recombinant HSP25 or HSP22 proteins can interrupt oligomer formation by the CryAB R120G.[30] The cardiomyopathy-causing αB-crystallin mutant R120G was found to be excessively phosphorylated, which disturbed survival of motoneuron (SMN) interaction and nuclear import, and resulted in the formation of cytoplasmic inclusions.[31]

The αB crystallin has strong antiapoptotic properties[39] and, when fully induced, may constitute as much as 5% of total cardiac myocyte.[6]A critical serine residue at position 59 of the αB crystallin protein that is targeted by the p38β-MAPKAP-K2 pathway during ischemic stress.[25,32] In apoptosis signal pathway, αB crystallin interacts with the procaspase-3 and partially processes procaspase-3 to repress caspase-3 activation. And αB crystallin prevents staurosporine-induced apoptosis through interactions with members of the Bcl-2 family.[8,22,23]

First of all, αB-crystallin has critical structural function in the rat cardiac myoblast cell line H9c2. When cytoskeleton was severely damaged by upon proteasome inhibition, αB crystallin was translocated from the detergent-soluble cytosolic fraction to the detergent-insoluble nuclear/cytoskeletal fraction. Indeed, phosphorylation of αB crystallin is not essential for the translocation.[10] Low-expression of αB crystallin with antisense cDNA in

glioma cells was found to lead to a disorganized microfilament network.[11] The studies about functions of αB crystallin have been conducted due to their powerful effect against various stresses in cells.

Recently, protein transduction domain (PTD) in a novel therapeutic perspective has been introduced to deliver target protein into cells directly.[12] One of PTDs is the human immunodeficiency virus (HIV-1) transactivator TAT protein. Among full amino acid of that, 11 amino acid (residues 47-57 of TAT) deliver a broad spectrum of proteins.[13] By using TAT protein, numerous target proteins can be delivered into cell. The interaction of TAT-PTD with cell surface causes the internalization of TAT-fusion proteins by lipid raft-dependent macropinocytosis.[14]

The most important object of our study is to develop a new powerful protein drug as PTD-fusion protein using PTD system. Protein drugs are expected as effective and strong drug, because they can affect specific targets directly, reduce the period of drug development, and have high safety better then drugs using target gene or chemical substances. Although PTD-fusion proteins entry into cell occurred quickly and affected target protein directly, it could be difficult to expect constant stability owing to protein properties. We found that matrix metalloproteinases (MMPs) are associated with degradation of PTD-fusion protein in cells. MMPs are a major group of enzymes that

regulate cell-matrix composition. And the MMPs are zinc-dependent endopeptidases known for their ability to cleave one or several ECM constituents, as well as non matrix proteins.[15,16,21] Several MMPs are expressed during wound healing, and mice deficient in MMP-3 and MMP-7 are defective in wound repair of the epidermis and trachea, respectively.[37,38] Interestingly, one of their functions is that the combination of TAT and MMP as a host defense mechanism produced significant attenuation of neurotoxicity through the degradation of TAT by MMP-1[18]. MMP-9 cleaves αB crystallin in autoimmune disease and Identified immunodominant and cryptic epitopes of αB crystallin in mice and rats were generated and largely left intact by MMP-9 processing.[20] These results indicates that MMPs can exert immune mechanism as well as enzyme activity that regulates cell-matrix composition and non matrix proteins.[18,20] In our study, we investigated the effect of TAT-αB crystallin fusion protein on the apoptotic stimulus in cardiac cells. We also analyzed the antiapoptotic pathway and degradation mechanism after transduction of TAT-αB crystallin into cells.

II. MATERIALS AND METHODS

1. Molecular cloning of human αB crystallin

The human αB crystallin cDNA was generated by PCR using human heart cDNA library (Clonetech, Palo Alto, CA, USA) as a template. To construct 6Xhis-TAT-HA-αB crystallin, the sense primer was 5'-CAC CTA CTC GAG ATG GAC ATC GCC ATC CAC-3' and the antisense primer was 5'-CAA GAA AGA ATT CCT ATT TCT TGG GGG CTG C-3'. The PCR product was digested with *Xho*I and *Eco*RI, and subcloned into the *Xho*I and *Eco*RI sites of the pTAT-HA bacterial expression vector (a gift from Dr. Stephen F. Dowdy, UCSD, USA). The pTAT-HA bacterial expression vector contains an N terminal 6-histidine tagging sequence, followed by the 11-amino acid transduction domain of the TAT protein. The correct sequence of the pTAT-HA-αB crystallin vector was confirmed by DNA sequencing using the universal T7 primer. To construct 6Xhis-αB crystallin, the sense primer was 5'-CTA GCC CAT ATG GAC ATC GCC ATC CAC CAC-3' and antisense primer was 5'-CAA GAA AGA ATT CCT ATT TCT TGG GGG CTG C-3'. The PCR product was digested with *Nde*-I and *Eco*RI and subcloned into the *Nde*-I and *Eco*RI sites of the pET28a bacterial expression vector. The pET28a bacterial expression vector contains an N-terminal 6-histidine tagging

sequence. The correct sequence of the pET28a-αB crystallin vector was confirmed by DNA sequencing using the universal T7 primer.

2. Expression and purification of αB crystallin fusion proteins

Escherichia coli BL21(DE3)pLysS (Novagen, Madison, WI, USA) was transformed with the pTAT-HA-αB crystallin plasmid, and then grown for overnight at 37℃ in LB broth supplemented with 100 μg/ml ampicillin and 34 μg/ml chloramphenicol. These cultures were diluted 100-fold with fresh LB media which was contained with 100 μg/ml ampicillin and 34 μg/ml chloramphenicol and cultured at 37℃ for 3 hr while shaking at 200 rpm. Protein expression was induced by the addition of 1 mM β-D-1-thiogalactopyranoside (IPTG) for 4 hr while shaking at 37℃. The TAT-αB crystallin fusion proteins were then isolated using a urea-denaturing protein purification protocol. The bacterial pellet was isolated by centrifugation at 7,000 rpm, washed with phosphated-burffed saline (PBS), resuspended in buffer Z (8 M urea, 100 mM NaCl and 20 mM HEPES, pH8.0), and sonicated on ice 5 times with 10 second pulses with 1mM phenylmethanesulphonyl-fluoride (PMSF). The sample was then clarified by centrifugation at 15,000 rpm at 4℃ for 30 min. The clarified lysate was loaded to Ni-NTA column at 1 ml/min, and then the column was washed using A buffer (50 mM NaH_2PO_4,

300 mM NaCl) for 1 hr at 1 ml/min. To elute TAT-αB crystallin, the column was loaded by using binding buffer containing increasing concentrations of imidazole (100-1,000 mM) at 1 ml/min. The protein concentrations in each fraction were quantified by the Bradford assay (BioRad, Hercules, CA, USA), using bovine serum albumin (BSA) as the standard. The purity of the fusion proteins was assessed by SDS-PAGE and Coomassie Brilliant blue staining. The purified fusion proteins dissolved in PBS containing 10% glycerol were aliquoted and stored at -80℃.

3. Animal cell culture

The rat heart-derived H9c2 cells were obtained from the American Type Culture Collection (ATCC, Rockville, MD, USA). H9c2 cells were cultured in Dulbecco's modified Eagle's medium/F-12 (DMEM/F-12) supplement with 10% FBS and 1% penicillin streptomycin (Gibco, Grand Island, NY, USA), at 37℃ in a humidified atmosphere of 5% CO_2 - 95% air. All experiments were performed using cells between passage numbers 11 and 20.

4. Transduction of TAT-αB crystallin fusion protein into cells

To transduce TAT-αB crystallin fusion proteins, cells were grown to confluence in 60 mm dish or 6-well plates. The culture medium was replaced

with fresh medium containing 10% FBS and was then treated with various concentrations of TAT-αB crystallin fusion proteins. The cells were washed with PBS, harvested by trypsinization for 5 min in order to remove TAT-αB crystallin binding cell membrane and fresh medium containing 10% FBS was added to inactivate trypsin. The cells were washed by using PBS for 3 times while centrifuged. Cells were prepared for analysis by immunoblot.

5. Immunoblot analysis

Protein-treated cells were washed once in PBS and lysed in a lysis buffer (Cell signaling, Beverly, MA, USA) containing 20 mM Tris (pH 7.5), 150 mM NaCl, 1 mM Na_2EDTA, 1 mM EGTA, 1% Triton, 2.5 mM sodium pyrophosphate, 1 mM β-glycerophosphate, 1 mM Na_3VO_4, 1 mg/ml leupeptin, and 1 mM PMSF. Protein concentrations were determined using the Bradford protein assay kit (BioRad, Hercules, CA, USA). Proteins were separated in a 15% or 12.5% SDS-polyacrylamide gel and transferred to poly-vinylidene difiuotide (PVDF) membrane (Millipore Co, Bedford, MA, USA). The membrane was blocked for 1 hr by 5% or 10 % non-fat dry Milk (BioRad). After blocking the membrane, it was washed 3 or 4 times with Tris-buffered saline-tween 20 (TBS-T, 0.1% tween 20) for 10 min at room temperature, and incubated with primary antibodies for 1 hr at room

temperature or for overnight at 4°C. The membrane was washed four times with TBS-T for 10 min, and then incubated for 1 hr at room temperature with horseradish peroxidase (HRP)-conjugated secondary antibodies. After extensive washing, the bands were detected by enhanced chemiluminescence (ECL) reagent (Santa Cruz Biotechnology, Santa Cruz, CA, USA).

6. Immunoprecipitation

Cell were washed once in PBS and lysed in a lysis buffer (Cell Signaling, Beverly, MA, USA) containing 20 mM Tris (pH 7.5), 150 mM NaCl, 1 mM Na_2 EDTA, 1 mM EGTA, 1% triton, 2.5 mM sodium pyrophosphate, 1 mM β-glycerophosphate**,** 1 mM Na_3VO_4, 1 mg/ml leupeptin and 1 mM PMSF. Protein concentrations were determined using Bradford protein assay kit (Bio Rad). Whole cell extract (200 μg) was pre-cleared with protein A/G agarose plus (Santa Cruz Biotechnology, Santa Cruz, CA ,USA) on a rotating platform plate at 4℃ for 2 hr and incubated with 2 μg of antibody on a rotating platform plate at 4℃ for overnight. Immunoprecipitation was facilitated by the addition of 15 μl of protein A/G agarose at 4℃ for 1 hr on a rotating platform plate. After serial washes for 3 times, it was subjected to SDS-PAGE and detected using immunoblot analysis.

7. Immunocytochemistry

Cells were grown on 4-well plastic dishes (SonicSeal Slide, Nalge Nunc, Rochester, NY, USA) and treated with various concentrating TAT-αB crystallin. Following incubation for 1 hr, the cells were washed twice with PBS and then fixed with methanol and ethanol (1:1 ratio) for 10 min at room temperature. The cells were washed again with PBS and then permeabilized for 15 min in PBS containing 0.2% triton. The cells were then blocked in PBS containing 5% BSA and then incubated for 1 hr with rabbit polyclonal histag alexa 647 antibody and FITC conjugated monoclonal Anti-β-Tubulin antibody. The cells were incubated with PBS containing 4',6-diamidino-2-phenlindde (DAPI) 0.02 μg/ml once and three times for 10 min with PBS. Confocal microscope (LSM 510 META, Carl Zeiss, Thornwood, New York, USA) was used for analysis.

8. Measurement of caspase-3 activity

The activity of caspase-3 in the H9c2 cells was determined spectrophotometrically with an Apoalert^{TM} CPP32/caspase-3 assay kit (BD Science, Palo Alto, CA, USA) by measuring the release of the chromophore, pnitroanilide (*p*NA), following hydrolysis of DEVD-*p*NA. H9c2 cells were incubated in DMEM without FBS and incubated with TAT-αB crystallin for 3

hr prior to treat 100 nM staurosporine for 2 hr. After then, cells were harvested, resuspended in chilled cell lysis buffer and incubated on ice for 10 min. Cells were centrifuged and supernatants were transferred to a fresh tube. Protein concentration was determined by the Bradford assay (BioRad, Hercules, CA, USA). The 50 µl of 2X reaction buffer containing 10 mM dithiothreitol (DTT) was added and each sample was incubated with 5 µl of DEVD-*p*NA (4 mM) at 37°C for 1 hr.

9. Matrix metalloproteinase cleavage assay

To test TAT-αB crystallin cleavage by MMPs, cleavage buffer (50 mM Tris (pH 7.5), 3 mM NaN_3, 5 mM $CaCl_2$, 1 µM $ZnCl_2$) was used. Recombinant TAT-αB crystallin (1 µg) was co-incubated with active MMP proteins in cleavage buffer for 2 hr at 37°C.

10. Preparation of detergent insoluble fraction

After cells were lysed with lysis buffer, the supernatants were transferred to new tube for soluble fraction. The remaining pellet was washed once with 500 µl of lysis buffer, and then centrifuged. The pellets were resuspended in 50 µl of lysis buffer.

11. Mitochondrial and cytoplasmic cell fractionation cytoplasmic cell fractionation

Mitochondrial and cytoplasmic fractionation was conducted by using the ApoAlert cell fractionation kit (BD Biosciences, Franklin Lakes, NJ USA) according to the manufacturer's instructions. The cells were centrifuged and removed supernatant, and then resuspended in 1 ml of ice-cold wash buffer, and centrifuged at 2,500 rpm for 5 min at 4℃. Once the supernatant was removed, the cells were resuspended in 200 μl of ice-cold fractionation buffer mix with protease inhibitor mixture and 1 mM dithiothreitol (DTT).

The tube was incubated on ice for 10 min, and the cells were passed through a device for homogenization about 20 times. They were transferred to new tube and centrifuged for 10 min at 4℃. Following centrifugation, the supernatant was transferred to a new tube and centrifuged at 10,000 rpm for 25 min at 4℃ to separate the cytosolic and mitochondrial fractions. The supernatant containing the cytoplasmic extract was transferred to a new tube, whereas the remaining pellet, which is the mitochondrial fraction, was resuspended in 200 μl of the fractionation buffer mix.

III. RESULTS

1. Construction and purification of αB crystallin fusion protein

To prepare cell-permeable αB crystallin fusion protein, the plasmid pHis-TAT-HA-αB crystallin was constructed as described in Materials and Methods (Fig. 1A). Competent *Escherichia coli* BL21 plysS was transformed with pHis-TAT-HA-αB crystallin and the protein was expressed in competent *Escherichia coli* BL21 plysS. The bacteria were cultured in LB medium with shaking (200 rpm) at 37℃ to a density of $O.D_{600}$ =0.6. Then, 1 mM IPTG was added in order to induce the expression of the recombinant proteins for 4 hr. Recombinant TAT-αB crystallin protein was purified by using Ni-NTA affinity column chromatography (Fig. 1B). This protein was analyzed by 12.5% SDS-PAGE and stained with Coomassie brilliant blue (Fig. 1C, D). And then the protein was dialyzed by using PBS. The purified protein was confirmed by immunoblot analysis with anti-αB crystallin antibody.

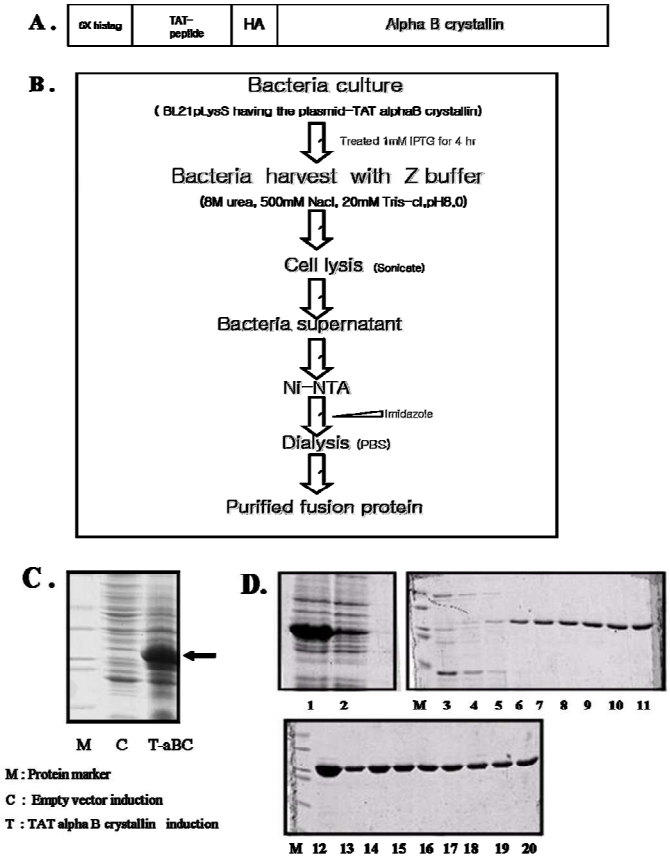

Fig. 1. Construction and purification of αB crystallin fusion protein. A. A schematic presentation of the αB crystallin containing His 6X tag-TAT-HA. TAT domain and αB crystallin-coding sequence were fused. B. Diagrammatic representation of protein purification. C. Recombinant TAT-αB crystallin in BL21 pLysS was induced by 1 mM IPTG. for 4 hr. D. TAT-αB crystallin was purified using Ni-NTA affinity chromatography. Coomassie brilliant blue stain was followed by purification of TAT-αB crystallin. Lane 1,2 present sample induced and flow through respectively, and lanes from 3 to 20 show continuous elution fraction

2. Transduction of TAT-αB crystallin into H9c2

To determine the efficiency of TAT-αB crystallin transduction, H9c2 cells were treated with TAT-αB crystallin for 2 hr and then removed media from the 4-well slide chamber. The cells were washed once with PBS-T and fixed with mixture of methanol and ethanol (1:1 ratio) for 10 min, and then permeabilized for 15 min in PBS containing 0.2% triton after being washed with PBS-T. The cells were incubated in PBS containing 5 % BSA for 1 hr in order to block the cells. The cells were rewashed three times for 10 min with PBS-T, and then incubated with Anti-HIS TAG-alexa 647 antibody for 1 hr. The intracellular TAT-αB crystallin was visualized using immuno-cytochemistry analysis (LSM 510 META, Carl Zeiss, Thornwood, New York, USA). As shown in Fig 2, these data presented that TAT-αB crystallin was effectively transduced across the plasma membrane and located in not only cytoplasm but also nucleus. The transduced TAT-αB crystallin proteins were almost located on cytoskeleton of H9c2 cell.

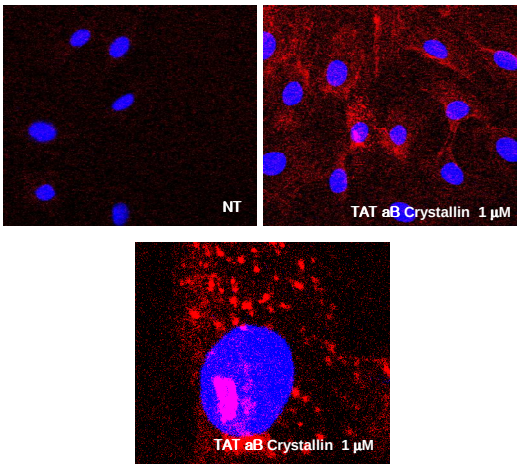

Fig. 2. An analysis of intracellular TAT-αB crystallin fusion proteins in H9c2 cells H9c2 cells were treated with 1 μM TAT-αB crystallin fusion proteins and stained with anti-HIS TAG-alexa 647 antibody and DAPI. The transduction of recombinant TAT-αB crystallin was observed by using confocal microscope.

3. Protective effect of TAT-αB crystallin in H9c2 cell

To explore the biological function of TAT-αB crystallin, the protein was added to cells for 2 hr before cells were treated with staurosporine from 1 to 100 nM for 3 hr. After that, the cells were observed with phase contrast microscope (CKX 41, OLYMPUS, Tokyo, Japan) (Fig. 3A). Although 10 nM or 100 nM staurosporine induced cell detachment or change of morphology, the cells which were pretreated with recombinant TAT-αB crystallin were recovered from staurosporine-induced cell death in same condition. These data showed the protective effect of TAT-αB crystallin in cardiac cell death-induced staurosporine. It had been reported various studies that over-expression of αB crystallin significantly affects protective function from cell damage related to apoptosis[8]. TAT-αB crystallin transduction is also powerful method to prevent the pathway caused staurosporine-induced apoptosis. The αB crystallin has also been reported to be particularly effective in stresses of cytoskeleton.[21] To confirm these protective effects, immunocytochemistry analysis was performed by using FITC conjugated monoclonal anti-β-Tubulin (Sigma, St. Louis, MO, USA) and anti-HIS TAG-alexa 647 antibody. The cells were incubated with TAT-αB crystallin or PBS for 3 hr and then treated with 0.01% DMSO or 100 nM staurosporine for 2 hr (Fig. 3B). As shown in Fig. 3B, severe disorganization of cytoskeleton was observed in the cells

which are incubated with only staurosporine 100 nM. In contrast, the cells which were transduced by TAT-αB crystallin did not display nuclear condensation as well as disorganization of cytoskeleton by staurosporine. Moreover, it was found that TAT-αB crystallin was co-located with cytoskeletons in staurosporine-induced cellular alteration. One of marked functions of αB crystallin is to repress depolymerization and aggregation of cytoskeletons by binding the site damaged directly.[10] As a result, TAT-αB crystallin transduction prevented cytoskeleton alteration from staurosporine-induced cell death and it could be expected as protein drug in cell death condition as staurosporine-induced apoptosis.

A.

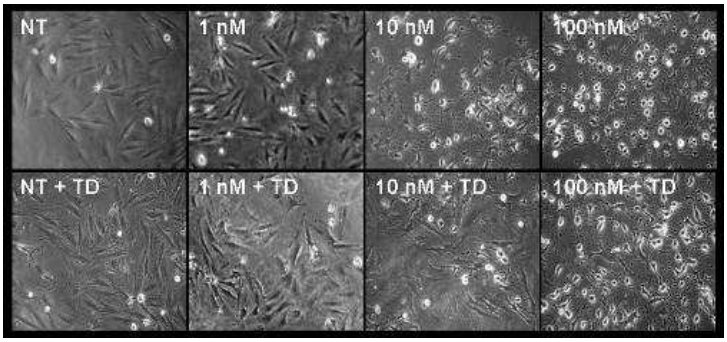

B.

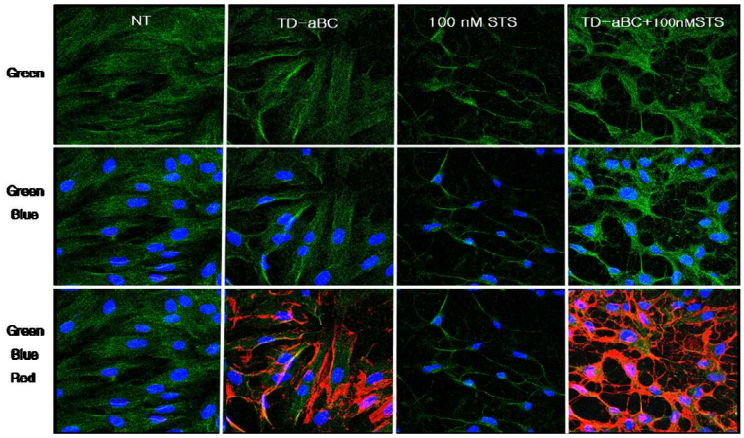

Fig. 3. Transduction of TAT-αB crystallin and its protective effect against staurosporine-induced cell death A. H9c2 cells were treated with 3 uM TAT-αB crystallin (TD) for 3 hr and then added to staurosporine of ranging from 1 nM to 100 nM for 2 hr. B. 5 uM TAT-αB crystallin was transduced to H9c2 cells which were pretreated with or without 100 nM staurosporine. Blue, green and red colors indicate nuclear, β-tubulin, TAT-αB crystallin respectively. NT (DMSO 0.01%), TD (TAT-αB crystallin 5 uM), STS 100 nM (staurosporine 100 nM), TD-aBC+STS 100 nM (TAT-αB crystallin 5 uM and staurosporine 100 nM)

4. Antiapoptotic effect of TAT-αB crystallin

Earlier studies have suggested that translocation of Bax directly induces cytochrome C to release from mitochondria to cytosol and caspase-3 activation.[8] To explore whether TAT-αB crystallin is able to prevent apoptosis at the mitochondria level and upstream of caspase-3 activation, it is examined for measurement of caspase-3 activity, interaction between Bax and αB crystallin, and cytochrome C translocation in order to identify possible antiapoptotic effect. To test the ability to repress cleavages of caspase-3 in apoptotic condition, H9c2 cells were co-incubated with TAT-αB crystallin for 3 hr, and then 100 nM staurosporine was treated to the cells for 2 hr. Caspase-3 activity was measured by using caspase-3 colormetric kit and immunoblot. The partial cleavages of caspase-3 decrease in the cells with TAT-αB crystallin (Fig. 4A) and total caspase-3 activity decreased by over 50% in the data using caspase-3 colorimetric kit (Fig. 4B).

To check prevention of staurosporine-induced cytochrome C release, the cells were incubated with TAT-αB crystallin and then treated with 0.01% DMSO or 20 nM staurosporine for 2 hr. The samples were harvested by using cytosolic and mitochondrial fraction method. Although all samples had a small amount of cytochrome C release, the data displayed a repressed tendency of their release by TAT-αB crystallin transduction. TAT-αB crystallin

also prevented release of cytochrome C from mitochodria to cytosol (Fig. 4C). Bcl-2 family members such as Bax are the major apoptotic regulator and they have been shown to be activated and translocated from the cytosol into mitochondria after apoptotic stimulation.[33] The αB crystallin binds to Bax and Bcl-xS to sequester their translocation during staurosporine-induced apoptosis.[8] To test whether TAT-αB crystallin is able to interact with Bax, we conducted immunoprecipitation analysis using anti-αB crystallin (Stressgen, Ann Arbor, Michigan,USA) and anti-Bax (Santa Cruz Biotechnology, Santa Cruz, CA, USA) antibody. The total proteins extracted from each sample were immunoprecipitated with anti-αB crystallin. The precipitated samples were then sequentially blotted with anti-Bax. As expected, TAT-αB crystallin interacted with Bax (Fig. 4D).

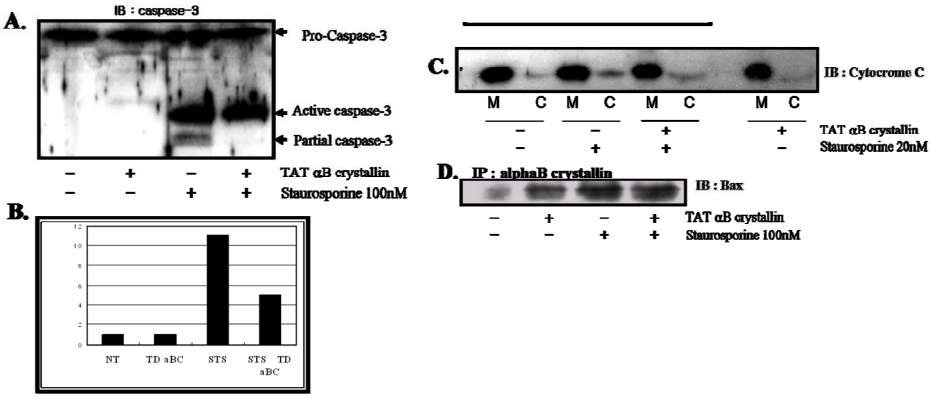

Fig. 4. TAT-αB crystallin prevents staurosporine-induced cytochrome C release and caspase-3 activation A. H9c2 cells were incubated with TAT-αB crystallin for 3 hr prior to the incubation of 100 nM staurosporine. The black arrows indicate active or inactive caspase-3 proteins, and the data was analyzed by anti-caspase-3 antibody. B. cells were harvested and same amount of cell extracts were used for caspase-3 assay. H9c2 cells were treated with 0.01% DMSO (DMSO) or 20 nM staurosporine (STS) for 2 hr after co-incubated with TAT-αB crystallin or PBS for 2 hr. These samples were then used for isolation of mitochondrial (M) and cytosolic (C) fractions. Total samples were then extracted from the two fractions using the ApoAlert cell fractionation kit. Anti-cytochrome C antibody was used for immunoblot analysis. D. this data indicates the interaction between TAT-αB crystallin and Bax during staurosporine-induced apoptosis or normal condition. H9c2 cells were incubated with TAT-αB crystallin for 3 hr, and then 100 nM staurosporine was treated to the cells for 2 hr. The cells were harvested for immunoprecipitation analysis.

5. The cleavage of the transduced TAT-αB crystallin in H9c2 cell

In protein transduction experiment using TAT-αB crystallin, the cleavage of TAT-αB crystallin was found during their transduction. (Fig. 5A,B) The H9c2 cells were incubated with 5 μM of TAT-αB crystallin for varying periods of time, and the amounts of protein taken up was analyzed by immunoblot using anti-αB crystallin antibody (Fig. 5A). As shown in Fig. 5A, TAT-αB crystallin entry increased in a time-dependent manner. The cleavages of transduced TAT-αB crystallin were displayed in 90 and 180 min and its level was eventually increased. The H9c2 cells were incubated with 1 μM or 5 μM of TAT-αB crystallin for 3 hr. the amounts of protein taken up and their cleavages were analyzed by immunoblot using anti-αB crystallin antibody. The cells which were incubated with 1 uM of TAT-αB crystallin did not showed small size among cleaved fragments of TAT-αB crystallin (Fig. 5B). These results demonstrate that TAT-αB crystallin protein could be delivered into cardiac H9c2 cells and be cleaved during transduction. To find out the reason these showed up, we tried to inhibit total activities of transcription, translation and proteasome during TAT-αB crystallin transduction by using actinomycin D, cyclohexamide and MG 132. But we did not find any difference in immunoblot result (not shown data).

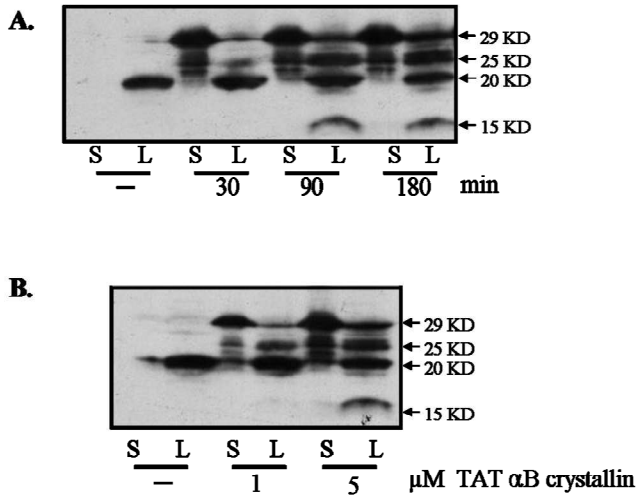

Fig. 5. Cleavage of transduced TAT-αB crystallin in H9c2 cell TAT-αB crystallin (5 uM) was transduced into H9c2 cells at time- or concentration-dependent manner. Media (M) and whole cell lysate (L) were prepared and immunoblot against αB crystallin were examined.

6. Different cleavage patterns of TAT-αB crystallin in soluble and insoluble fraction of cells

In order to know the tendency in detail, we explored the patterns of TAT-αB crystallin transduction and the cleavages of intracellular TAT-αB crystallin at concentration- and time-dependent manner. TAT-αB crystallin was added to H9c2 cells at concentration ranging from 1 μM to 10 μM for 3 hr or time ranging from 30 to 720 min. These samples were then used for isolation of soluble and insoluble fractions. Protein samples were then extracted from the two fractions. The amounts of transduced proteins were analyzed by immunoblot using anti-αB crystallin antibody. TAT-αB crystallin was successfully transduced at 5 μM concentration (Fig. 6A upper panel) and the small band of TAT-αB crystallin became to appear by 5 μM TAT-αB crystallin. As shown in Fig. 6 B, TAT-αB crystallin entry rapidly occurred at time-dependent manner. And the cleaved bands of 15 kD were highly generated from 60 to 120 min, after that, disappeared by degrees. Through these results, we could expect that the cleavage and insolubilization in TAT-αB crystallin transduction is one of the mechanisms related to protein degradation. Therefore, we also investigated insoluble fraction of that experiment in order to know whether TAT-αB crystallin cleavages affected their degradation. As shown in Fig 6B, the small fragments of cleaved TAT-αB crystallin happened

in 60 min. After that, they gradually increased in total insoluble protein. Therefore, the loss of function of intracellular TAT-αB crystallin in cells was accelerated by their cleavage. Interestingly, non-cleaved TAT-αB crystallin (29 kD) located in insoluble fraction better than soluble fraction.

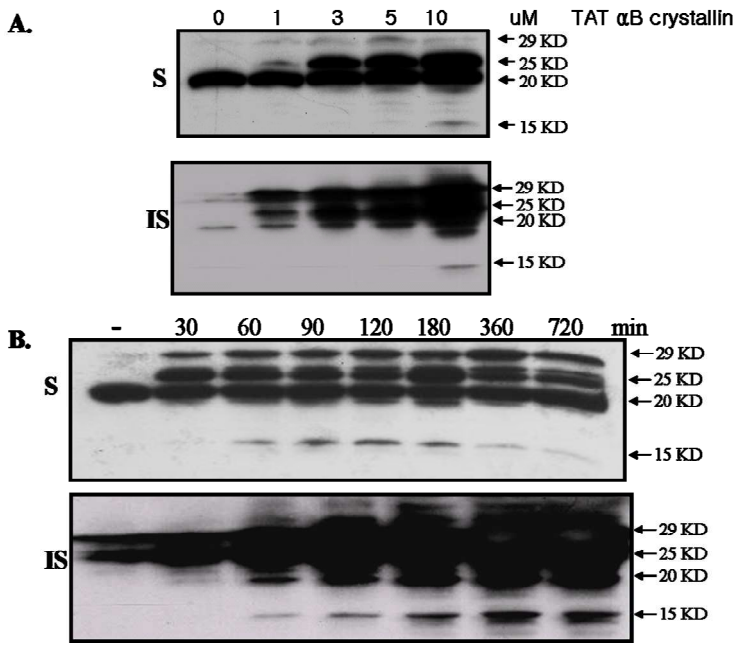

Fig. 6. Concentration- and time-dependent transduction of TAT-αB crystallin and different cleavage patterns between soluble and insoluble fraction A. TAT-αB crystallin was transduced into H9c2 cell at various concentrations and indicated time. Cells were incubated with 1 μM, 3 μM or 5 μM TAT-αB crystallin for 1 hr. The samples were isolated to soluble (S) and insoluble (IS) fraction by detergent insoluble fraction method. B. TAT-αB crystallin transduction into H9c2 cell at time-dependent manner. Cells were incubated with TAT-αB crystallin (5 uM) for ranging from 30 to 720 min.

7. Cleavages of TAT-αB crystallin by matrix metalloproteinase-1

We hypothesized that the proteins having endopeptidase activity could attack intracellular TAT-αB crystallin. In the previous study, it has been reported that cleavage of HIV-TAT is related to MMPs.[18] To determine whether MMP-1 could directly interact with TAT-αB crystallin, TAT-αB crystallin was incubated with MMP-1 in MMP reaction buffer and analyzed them by Coomassie blue staining and immunoblot (Fig. 7A,B). MMP-1 cleaved TAT-αB crystallin, as demonstrated by disappearance of the TAT-αB crystallin band and appearance of low size band from the gel. Furthermore, when FN-439, which is an MMP-1 inhibitor, was added to the reaction mixture, the cleavage of TAT-αB crystallin band reappeared (Fig. 7C).

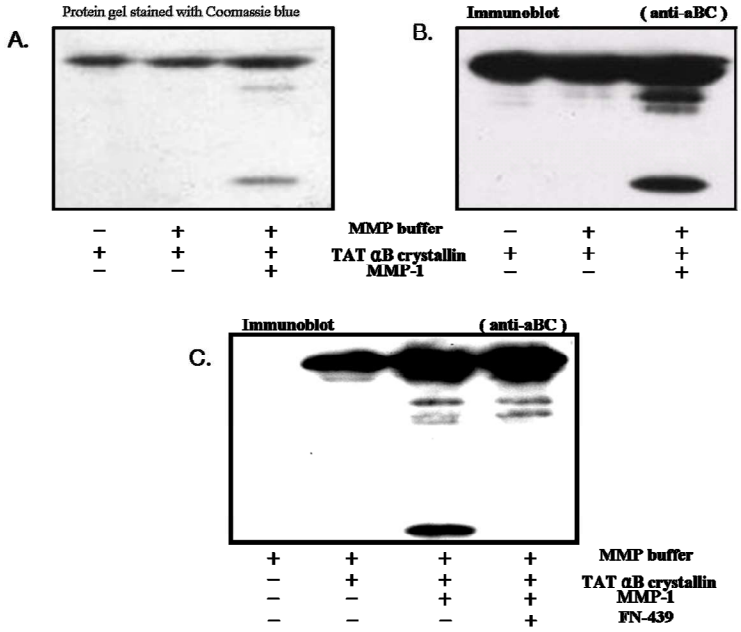

Fig. 7. Specific cleavage of TAT-αB crystallin by MMP-1 Cleavage of TAT-αB crystallin is specific to the endopeptidase activity of MMP-1. TAT-αB crystallin was co-incubated with MMP-1 at 37°C for 2 hr. Reaction products were separated by SDS-PAGE and analyzed by Coomassie blue staining (A) and immunoblot (B,C). MMP-1 inhibitor (FN-439) was pre-incubated with MMP-1 for 30 min and then TAT-αB crystallin was added (C).

8. Cleavage of recombinant αB crystallin and TAT-αB crystallin by matrix metalloproteinase-1

Based on these results, we needed to know whether the reaction between TAT-αB crystallin and MMP-1 is specialized by TAT peptide. We constructed the plasmid pHis–αB crystallin as described in Materials and Methods and then αB crystallin was purified by Ni-NTA affinity column chromatography (Fig. 8A). To know correlation between TAT peptide and MMP-1, recombinant αB crystallin (TAT free) was co-incubated with MMP-1 *in vitro*, and TAT-αB crystallin was also used for control in this experiment. This data displayed the small size bands derived from αB crystallin. Therefore, there was no relation to TAT peptide in the reaction between MMP-1 and αB crystallin. These bands were same bands derived from TAT-αB crystallin. But we could also see another clear protein band around 25 kD from SDS-polyacrylamide gel stained with Coomassie brilliant blue and Western blot data in the reaction between MMP-1 and TAT-αB crystallin. From this result, we anticipated that TAT peptide residue of TAT-αB crystallin was cleaved or degraded by MMP-1, because anti-αB crystallin antibody recognizes C-terminal sequence (REEKPAVTAAPKK) within TAT-αB crystallin. From analysis of total amino acid sequence, this result indicated that MMP-1 could directly cleave or digest both in the middle of TAT-αB crystallin and TAT

peptide *in vitro*.

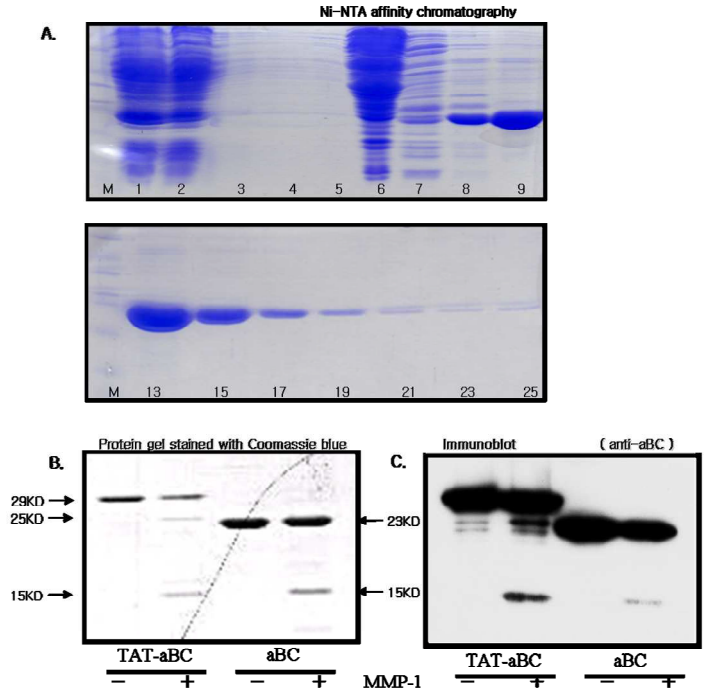

Fig. 8. Cleavage of recombinant αB crystallin and TAT-αB crystallin by MMP-1 A. Recombinant αB crystallin protein was purified using the Ni-NTA affinity column chromatography. B. Two types of recombinant αB crystallin were incubated with MMP-1. The data were analyzed by Coomassie blue gel staining (B) and immunoblot (C).

9. Cleavages patterns of TAT-αB crystallin by various matrix metalloproteinases

To extend our study to find new functions of other MMPs in TAT-αB crystallin cleavage, we prepared recombinant MMP-1,-3,-7,-8,-9 proteins, and conducted previous experiments about cleavage patterns by using other MMPs. Coomassie blue gel staining (Fig. 9A) and immunoblot (Fig. 9B) method was used for analysis. As shown in Fig 9, MMP-1,-8,-9 had the endopeptidase activity at same peptide domain within TAT-αB crystallin. Uniquely, TAT-αB crystallin was quickly degraded in the cleavage reaction with MMP-7. MMP-7 had strong endopeptidase activity at total peptide domain of TAT-αB crystallin. Interestingly, MMP-3 solely affected unique cleavage of TAT-αB crystallin in these reactions.

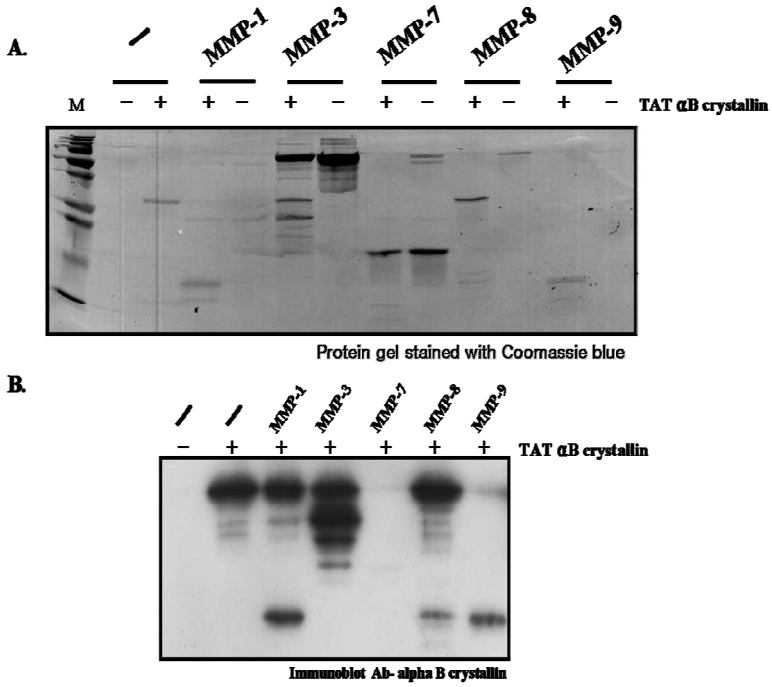

Fig. 9. Cleavage patterns of TAT-αB crystallin by MMPs TAT-αB crystallin was co-incubated with various MMPs for 2 hr. Immunoblot and Coomassie blue method were used for exact analysis.

10. Cleavage site within TAT-αB crystallin by matrix metalloproteinases

To know exact amino acid sequence of fragments cleaved by MMP-1 and MMP-3, TAT-αB crystallin of 10 μg was used for N-terminal amino acid sequencing analysis. TAT-αB crystallin was incubated with MMP-1 or MMP-3 for 2 hr. As shown in Fig. 10B, black arrow indicates major cleaved bands. This band was used for protein sequencing system. The result of TAT-αB crystallin cleavage site was described in Fig. 10A. The N-terminal sequences of a major fragment of TAT-αB crystallin in MMP-1 reaction were determined to be LRAPS (leucine, arginine, alanine, proline, serine), and the N-terminal sequences of a major fragment of TAT-αB crystallin in MMP-3 reaction were determined to be GGSTM (glycine, glycine, serine, threonine, methionine). We noticed that MMP-1 and MMP-3 mainly cleaved the domain within αB crystallin and TAT domain respectively. It is interesting to note that MMP-3 has endopeptidase activity at TAT domain of TAT-αB crystallin protein and MMP-1,-8,-9 have endopeptidase activity at specific site of TAT-αB crystallin protein.

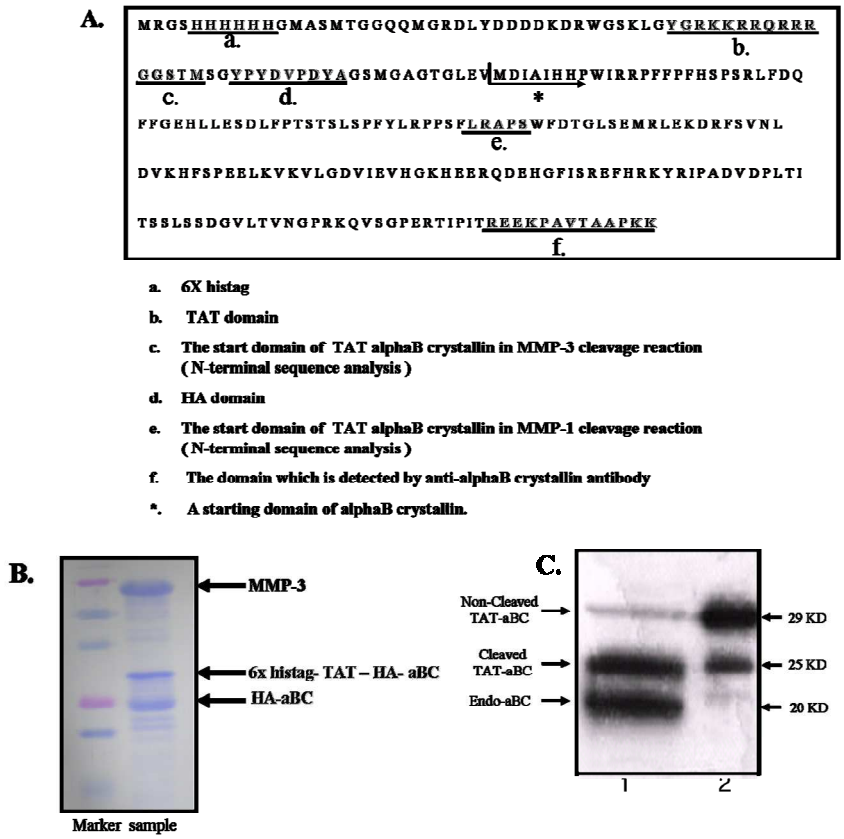

Fig. 10. An analysis of MMP-1, -3 cleavage site within TAT-αB crystalline by MMPs A. Demonstration of cleavage site of TAT-αB crystallin by MMP-1,-3. B. TAT-αB crystallin was incubated with recombinant MMP-1 or MMP-3 for 2 hr. The samples were separated by SDS-PAGE and then transferred to PVDF membrane. The membranes were stained with Coomassie blue solution. Major bands were separated from total membrane and analyzed by Procise 492 cLC protein sequencer (Applied Biosystems, USA). C. Comparison of cleavage TAT-αB crystallin between in cell and in tube. (1, TAT-αB crystallin transduction into H9c2 cells; 2, TAT-αB crystallin cleavage by MMP-3 in tube).

11. Time-dependent cleavage of TAT-αB crystallin by matrix metalloproteinases

To examine the patterns of TAT-αB crystallin degradation, TAT-αB crystallin was incubated for 0-360 min with MMP-1, MMP-3, MMP-7, MMP-8 and MMP-9 *in vitro*, respectively (Fig.11). TAT-αB crystallin (0.2 ㎍) was used for this test. Cleavage patterns of TAT-αB crystallin by MMPs were measured by immunoblot analysis. The samples treated with MMP-1 or MMP-9 showed that same pattern was displayed, and another sample incubated with only MMP-3 displayed that totally different pattern appeared in comparison with MMP-1 and MMP-9. The intact form of TAT-αB crystallin was almost degraded at 360 min in incubation with MMP-1, MMP-3 and MMP-8. Surprisingly, the intact form of TAT-αB crystallin was completely degraded only in 30 min incubation with MMP-7. MMP-8 hardly affected TAT-αB crystallin degradation in MMP reaction.

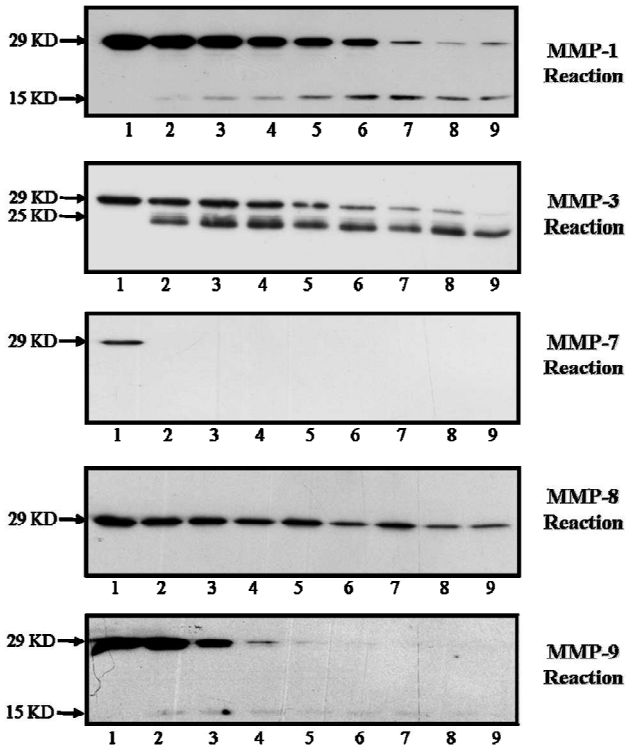

Fig. 11. Time-dependent cleavage of TAT-αB crystallin by MMPs TAT-αB crystallin were incubated for 0-360 min with MMP-1,-3,-7,-8, or -9 at 37℃(1, 0 min; 2, 30 min; 3, 60 min; 4, 90 min; 5, 120 min; 6, 180 min; 7, 240 min; 8, 300 min; 9, 360 min).

12. Effect of matrix metalloproteinases inhibitors on the cleavage of TAT-αB crystallin

Cells were pretreated for 1 hr with MMP inhibitor which could inhibit MMP-1, MMP-3 and MMP-7 broadly and then incubated with 5 uM TAT-αB crystallin for 1 hr. The cells were isolated to soluble and insoluble fraction by detergent insoluble fraction method. And anti-αB crystallin antibody was used for pattern analysis. As shown in Fig. 12, a great number of transduced TAT-αB crystallin became located in insoluble state, although intracellular TAT-αB crystallin generally maintained soluble state in H9c2 cell. But this tendency attenuated in the cells which were incubated with MMP inhibitor. This data indicated that MMP inhibitor was able to improve the quantity of active intracellular TAT-αB crystallin and decreased the degradation of transduced TAT-αB crystallin.

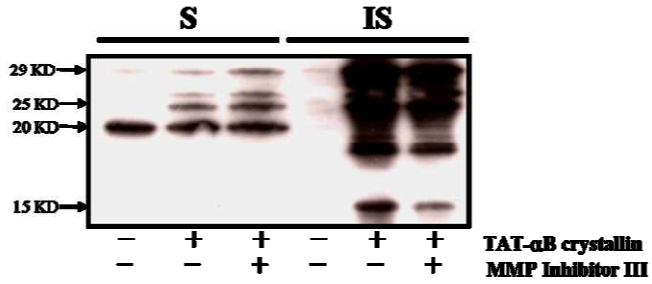

Fig. 12. Effect of solubility of TAT-αB crystallin by MMP inhibitor Cells were starved for 24 hr and then treated for 1 hr with MMP inhibitor 150 nM (MMP Inhibitor III, Calbiochem), and then TAT-αB crystallin (5 uM) was incubated for 1 hr. (S : soluble fraction, IS : insoluble fraction)

13. Suppression of cleavage of TAT-αB crystallin by the inhibitors of MAP kinases and matrix metalloproteinases

Previous our data have showed that the cleavage of transduced TAT-αB crystallin occurred quickly. Hence, we further explored the relation between transduced TAT-αB crystallin and MMPs. MMPs are regulated through MAPK and AP-1 pathways in fibroblasts,[19] and HIV-TAT protein activates c-Jun N-terminal kinase and activator protein-1.[17] To test whether the increased MMP endopeptidase activity was followed by MAP kinase in TAT-αB crystallin transduction, we performed the experiment using MAPKase inhibitor in TAT-αB crystallin transduction. The cells were pretreated with MAP kinase inhibitors such as p38, JNK and ERK for 1 hr, and 3 uM TAT-αB crystallin was added. As shown in Fig. 13, when the cell were pretreated with JNK inhibitor, the non-cleaved band (29 kD) of TAT-αB crystallin increased as well as that of the cleaved band (25 kD) decreased. ERK inhibitor and MMP inhibitor also affected the quantity of non-cleaved TAT-αB crystallin (29 kD), although barely altering the quantity of the cleaved TAT-αB crystallin (25 kD). The result suggested that JNK pathway was mainly associated with MMP endopeptidase activity in TAT-αB crystallin transduction. But the pathway of p38 MAPK pathway was hardly related in TAT-αB crystallin cleavage.

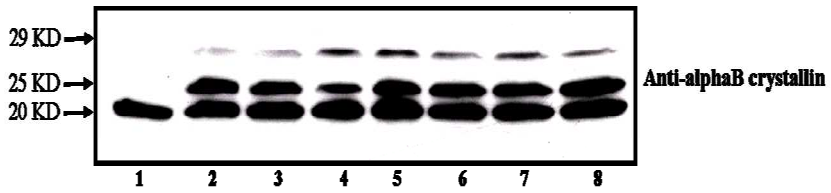

Fig. 13. Effect of MAP kinase inhibitors on the cleavage of TAT-αB crystallin 1, DMSO 0.01%; 2, only TAT-αB crystallin; 3, p38 inhibitor and TAT-αB crystallin; 4, JNK inhibitor and TAT-αB crystallin; 5, ERK inhibitor and TAT-αB crystallin; 6, MMP-1, -7 inhibitor and TAT-αB crystallin; 7, MMP-3 inhibitor and TAT-αB crystallin. The cells were starved with serum-free media for 24 hr and pre-incubated with inhibitors or DMSO for 30 min, and then co-incubated with TAT-αB crystallin (3 uM) for 2 hr.

14. Activation of Jun N-terminal kinase and matrix metalloproteinase-3 by TAT-αB crystallin transduction in cells

To gain further insight into the role of JNK pathway in the TAT-αB crystallin cleavage by MMP-3, we investigated JNK and MMP-3 activity during TAT-αB crystallin transduction. After starvation for 24 hr, the cells were incubated with TAT-αB crystallin at time- or concentration- dependent manner. To determine that the constitutive JNK activation is due to TAT-αB crystallin transduction, the cells were incubated with 3 uM TAT-αB crystallin for time ranging from 10 to 150 min (Fig. 14A). Quantitative variations of SAPK/JNK and SAPK/JNK phosphorylation were measured by immunoblot, and anti-β-actin antibody was used as standard. As shown in Fig. 14A, JNK phosphorylation was remarkably detected only in early 20 min, and the total protein level of constitutive JNK did not changed. We next investigated active MMP-3 protein and JNK phosphorylation level at concentration-dependent manner of TAT-αB crystallin. The cells were incubated with TAT-αB crystallin of concentration ranging from 100 nM to 5 uM for 1 hr (Fig. 14B). Quantitative variations of MMP-3 and SAPK/JNK phosphorylation were measured by immunoblot, and anti-β-actin antibody was used as standard. As shown in Fig. 14B, the protein level of active MMP-3 increased gradually at concentration-dependent manner.

A.

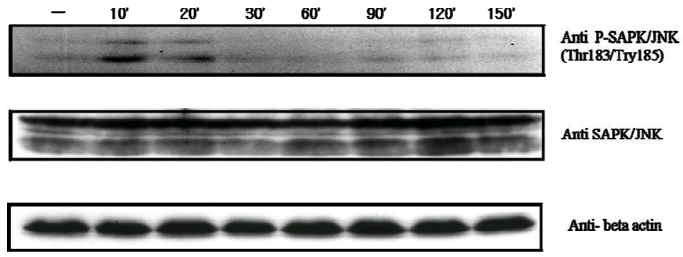

B.

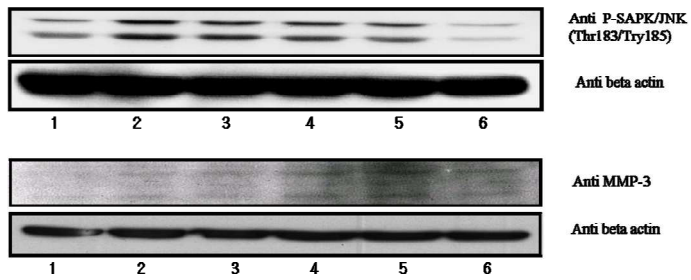

Fig. 14. TAT-αB crystallin transduction induces MMP-3 and JNK activation in cells A. After starvation for 24 hr, the cells were incubated with TAT-αB crystallin for 10-150 min. B. Cells were co-incubated with TAT-αB crystallin of ranging from 100 nM to 5 uM after starved for 24 hr (1, PBS; 2, TAT-αB crystallin 100 nM; 3, TAT-αB crystallin 500 nM; 4, TAT-αB crystallin 1 uM; 5, TAT-αB crystallin 3 uM, 6, TAT-αB crystallin 5 uM).

IV. DISCUSSION

This study demonstrated that intracellular delivery of αB crystallin protein fused to a protein transduction domain TAT showed significant protective effect against staurosporine–induced apoptosis and MMPs affected the cleavage of intracellular TAT-αB crystallin during transduction. We first produced αB crystallin containing the 11-amino acid transduction domain of TAT using recombinant technology. The TAT-αB crystallin fusion protein could enter efficiently H9c2 cells (Fig. 2).

Previous other studies demonstrated that αB crystallin exert significant protective effect against staurosporine-induced apoptosis in H9c2 cell.[8] It has been reported to interacting with the Bcl-2 family and cytochrome C as well as the procaspase-3 and partially process procaspase-3 to repress caspase-3 activation in order to block apoptosis.[8,39,40,41,44] Recently, the protein transduction domains (PTDs) including TAT represents a potentially valuable tool for the treatment of several diseases.[34,45,46,47]

In this study, using protein delivery system, we dealt with the antiapoptotic effect of TAT-αB crystallin in staurosporine–induced apoptosis and its cleavage mechanism by MMPs during transduction. Our data also showed that TAT-αB crystallin transduction improved strong antiapoptotic

effect similar to over-expression of αB crystallin in noxious stress. They prevented cytochrome C release and caspase-3 activation, and interacted with Bax in staurosporaine–induced apoptosis. These results suggest that TAT-αB crystallin could be possible to be used as clinical protein drug. Especially, TAT-αB crystallin was totally collocated in the cytoskeleton which was damaged by staurosporine. Intriguingly, disruption of the cytoskeleton and disaggregation of actin fibers are among the most immediate effects of heat shock in higher eukaryotes[32] and the stability of the actin filaments is considered as an important factor in the survival of cells exposed to hyperthermia and other stresses.[21] Disassembly or disturbance of the components of the cytoskeletal network result in the activation of convergent pathways to MAPK p38 pathways, which results in the phosphorylation of αB crystallin and changes in its localization.[21,48,49] The αB crystallin has critical structural function in the rat cardiac myoblast cell line.[10] when cytoskeleton is severely damaged by upon proteasome inhibition, αB crystallin is translocated from the detergent-soluble cytosolic fraction to the detergent-insoluble nuclear/cytoskeletal fraction, however, phosphorylation of αB crystallin is not essential for the translocation.[10,50] As shown Fig. 3B, TAT-αB crystallin prevented nuclear condensation as well as disorganization of cytoskeleton from staurosporine by binding damaged site directly.

In the present study, we observed that, after TAT-αB crystallin was transduced into H9c2 cell, it was cleaved (Fig. 5,6) and MMPs directly interacted with TAT-αB crystallin *in vitro* (Fig. 7-9). MMPs are a major group of enzymes that regulate cell-matrix composition.[15,16,43] When MMP-3 or JNK inhibitor was pretreated, the cleavage of intracellular TAT-αB crystallin was attenuated in H9c2 cells (Fig. 13). In previous studies related to MMPs and HIV-Tat, the interaction between MMP-1 and TAT protein could occur and the combination as a host defense mechanism produced significant attenuation of neurotoxicity through the degradation of Tat by MMP-1.[18] Interestingly, it was not observed the tendencies when low concentration (< 1 uM) of TAT-αB crystallin was added to cells (not shown data). Therefore, we hypothesized that these patterns were considered as one of defense mechanisms for cells and as a reaction for maintaining intracellular homeostasis, because the cells might need to remove excessive proteins because of sudden increase of specific protein in cell. But it was difficult to expect antiapoptotic effect at low concentration (< 1 uM) of TAT-αB crystallin. Hence, we had no choice but to treat high concentration of TAT-αB crystallin.

Although we pretreated preteasome inhibitor (MG 132), the cleavage band was not decreased. On the other word, MMPs might be associated with early degradation of intracellular TAT-αB crystallin rather than proteasomal

degradation in protein delivery system. As shown in Fig. 6C and 6D, the cleaved bands about 15 kD were strongly generated from 60 to 120min, and then disappeared by degrees. In contrast, the cleaved fragments in insoluble fraction appeared in 60 min and then increased gradually. Through these data, we could expect that the cleavage is concerned with an early stage of their degradation in TAT-αB crystallin transduction.

In another study related to the cleavage of αB crystallin, MMP-9 can cleave αB crystallin in autoimmune disease. Identified immunodominant and cryptic epitopes of aB crystallin in mice and rats were generated and largely left intact by MMP-9 processing.[20] In this study, we found new mechanism that TAT-αB crystallin is cleaved by MMP-1,-3,-7,-8,-9 directly *in vitro*. Until now, few papers have been published on cleavage relating between αB crystallin and MMPs. The cleavage patterns *in vitro* of TAT-αB crystallin by MMPs are similar to that of transduced TAT-αB crystallin.

MMP function is regulated through MAPK and AP-1 pathways,[19,42,43] and HIV-TAT protein activates JNK and activator protein-1 (AP-1).[17] We had tried to repress the function of MMPs by using MAPKase or MMP inhibitors, and when we pretreated JNK inhibitor in the cells, the cleavage patterns of intracellular TAT-αB crystallin were considerably changed (Fig. 13), and the signal pathway related to JNK and MMPs were activated by TAT-αB

crystallin transduction (Fig. 14). Active MMP-3 activates various MMPs such as MMP-1, MMP-2, MMP-7, MMP-8 and MMP-9.[27] Therefore, the generation of 15 kD can be considered as MMP-3 activation.

In protein delivery system, one of the disadvantages is low stability in cells because of proteins were degraded by proteasome. The ubiquitin-proteasome system is the major extra-lysosomal pathway for controlled degradation of intracellular proteins in eukaryotes. It generally plays a key role in protein degradation.[35] The problem of protein degradation has been considered many times over the past years. If it was solved, protein delivery therapy could be used as more powerful therapy. Through our results, we knew that MMPs could cleave TAT-αB crystallin through recognizing TAT domain and specific amino acid sequence within αB crystallin, and they were highly associated with the degradation of intracellular TAT-αB crystallin. We hypothesized that the stability of intracellular TAT-αB crystallin could be extended through control of MMP and JNK activity. Interestingly, as shown in Fig. 5, intracellular non-cleaved TAT-αB crystallin (29 kD) located in insoluble fraction rather than soluble fraction, and besides intracellular cleaved TAT-αB crystallin (25 kD) mainly located in soluble state in cell. It seems that cleaved TAT-αB crystallin (25 kD) is more stable in cell. After all, MMP-3 could assist intracellular TAT-αB crystallin to advance the stability

through removing TAT domain. Now, we are further studying about relationship between MMPs and the stability of intralcellular TAT-αB crystallin.

In conclusion, we have demonstrated the following: (1) TAT-αB crystallin fusion protein could enter efficiently H9c2 cells; (2) TAT-αB crystallin has strong antiapoptotic effect in staurosporine-induced apoptosis such as the repression of cytochrome C release, binding to Bax and inhibition of caspase-3 activity; (3) TAT-αB crystallin is cleaved during transduction; (4) recombinant MMP-1,-3,-7,-8,-9 proteins can cleave TAT-αB crystallin and recombinant αB crystallin; (5) MMP-3 has endopeptidase activity at TAT domain within TAT-αB crystallin protein and MMP-1,-8,-9 have endopeptidase activity at specific site within αB crystallin protein.; (6) the transduction of TAT-αB crystallin activates JNK and MMP-3; (7) through inhibition of MMP-3 and JNK activity, the cleavage of intracellular TAT-αB crystallin is attenuated. These results suggest that TAT-αB crystallin transduction could be expected as protein drug in cell death condition and that MMPs could be a key role in the stability of intracellular TAT-αB crystallin.

V. REFERENCE

1. Pandey P, Farber R, Nakazawa A, Kumar S, Bharti A, Nalin C, Weichselbaum R, Kufe D, Kharbanda S. Hsp27 functions as a negative regulator of cytochrome c-dependent activation of procaspase-3. Oncogene 2000; 19: 1975-81.

2. Garrido C, Bruey JM, Fromentin A, Hammann A, Arrigo AP, Solary E. HSP27 inhibits cytochrome c-dependent activation of procaspase-9. FASEB J 1999; 13: 2061-70.

3. Bruey JM, Ducasse C, Bonniaud P, Ravagnan L, Susin SA, Diaz-Latoud C, Gurbuxani S, Arrigo AP, Kroemer G, Solary E, Garrido C. Hsp27 negatively regulates cell death by interacting with cytochrome c. Nat Cell Biol 2000; 2: 645-52.

4. MacRae T. H. Structure and function of small heat shock/a-crystallin proteins: established concepts and emerging ideas. Cell. Mol. Life Sci 2000; 57: 899-913

5. van den IJssel P, Norman DG, Quinlan RA. Molecular chaperones: small heat shock proteins in the limelight. Curr Biol 1999; 9: R103-5.

6. Bishopric NH, Andreka P, Slepak T, Webster KA. Molecular mechanisms of apoptosis in the cardiac myocyte. Curr Opin Pharmacol 2001; 1: 141-50.

7. Morrison LE, Hoover HE, Thuerauf DJ, Glembotski CC. Mimicking phosphorylation of alphaB-crystallin on serine-59 is necessary and sufficient to provide maximal protection of cardiac myocytes from apoptosis. Circ Res 2003; 92: 203-11.

8. Mao YW, Liu JP, Xiang H, Li DW. Human alphaA- and alphaB-crystallin bind to Bax and Bcl-X(S) to sequester their translocation during staurosporine-induced apoptosis. Cell Death Differ 2004; 11:512-26.

9. Taylor R. P. and Benjamin I. V. Small heat shock proteins: a new classification scheme in mammals. J. Mol. Cell Cardiol 2005; 38: 433–44.

10. Verschuure P, Croes Y, van den IJssel PR, Quinlan RA, de Jong WW, Boelens WC. Translocation of small heat shock proteins to the actin

cytoskeleton upon proteasomal inhibition. J Mol Cell Cardiol. 2002 ; 34: 117-28.

11. Iwaki T, Iwaki A, Tateishi J, Goldman JE. Sense and antisense modification of glial alpha B-crystallin production results in alterations of stress fiber formation and thermoresistance. J Cell Biol. 1994; 125:1385-93.

12. Noguchi H, Matsumoto S. Protein transduction technology: a novel therapeutic perspective. Acta Med Okayama. 2006; 60: 1-11.

13. Becker-Hapak M, McAllister SS, Dowdy SF. TAT-mediated protein transduction into mammalian cells. Methods. 2001; 24: 247-56.

14. Wadia JS, Stan RV, Dowdy SF. Transducible TAT-HA fusogenic peptide enhances escape of TAT-fusion proteins after lipid raft macropinocytosis. Nat Med. 2004; 10: 310-5.

15. Massova I, Kotra LP, Fridman R, Mobashery S. Matrix metalloproteinases: structures, evolution, and diversification. FASEB J

1998; 12:1075-95.

16. McCawley LJ, Matrisian LM. Matrix metalloproteinases: they're not just for matrix anymore! Curr Opin Cell Biol 2001; 13: 534-40.

17. Kumar A, Manna SK, Dhawan S, Aggarwal BB. HIV-Tat protein activates c-Jun N-terminal kinase and activator protein-1. J Immunol 1998; 161:776-81.

18. Rumbaugh J, Turchan-Cholewo J, Galey D, St Hillaire C, Anderson C, Conant K, Nath A. Interaction of HIV Tat and matrix metalloproteinase in HIV neuropathogenesis: a new host defense mechanism. FASEB J. 2006; 20: 1736-8.

19. Kajanne R, Miettinen P, Mehlem A, Leivonen SK, Birrer M, Foschi M, Kähäri VM, Leppä S. EGF-R regulates MMP function in fibroblasts through MAPK and AP-1 pathways. J Cell Physiol 2007; 212: 489-97.

20. Starckx S, Van den Steen PE, Verbeek R, van Noort JM, Opdenakker G. A novel rationale for inhibition of gelatinase B in multiple sclerosis: MMP-9

destroys alpha B-crystallin and generates a promiscuous T cell epitope. J Neuroimmunol 2003; 141: 47-57.

21. Launay N, Goudeau B, Kato K, Vicart P, Lilienbaum A. Cell signaling pathways to alphaB-crystallin following stresses of the cytoskeleton. Exp Cell Res 2006 ; 312: 3570-84.

22. Susin SA, Zamzami N, Castedo M, Hirsch T, Marchetti P, Macho A, Daugas E, Geuskens M, Kroemer G.. Bcl-2 inhibits the mitochondrial release of an apoptogenic protease. J Exp Med 1996; 184: 1331-41.

23. Dole MG, Clarke MF, Holman P, Benedict M, Lu J, Jasty R, Eipers P, Thompson CB, Rode C, Bloch C, Nunez and Castle VP. Bcl-xS enhances adenoviral vector-induced apoptosis in neuroblastoma cells. Cancer Res1996; 56: 5734–40.

24. Laksanalamai P. and Robb F. T. Small heat shock proteins from extremophiles. Extremophiles 2004; 8: 1–11.

25. Ito H, Kamei K, Iwamoto I, Inaguma Y, Nohara D, Kato K.

Phosphorylation-induced change of the oligomerization state of alpha B-crystallin. J Biol Chem 2001; 276:5346–52.

26. Dalle-Donne I, Rossi R, Milzani A, Di Simplicio P, Colombo R. The actin cytoskeleton response to oxidants: from small heat shock protein phosphorylation to changes in the redox state of actin itself. Free Radic Biol Med 2001; 31:1624-32.

27. Chakraborti S, Mandal M, Das S, Mandal A, Chakraborti T. Regulation of matrix metalloproteinases: an overview. Mol Cell Biochem 2003; 253: 269-85.

28. Somasundaram T, Bhat SP. Canonical heat shock element in the alpha B-crystallin gene shows tissue-specific and developmentally controlled interactions with heat shock factor. J Biol Chem. 2000; 275: 17154-9.

29. Vicart, P., Caron, A., Guicheney, P., Li, Z., Prevost, M. C., Faure, A., Chateau, D., Chapon, F., Tome, F., Dupret, J. M., Paulin, D., and Fardeau, M. A missense mutation in the alphaB-crystallin chaperone gene causes a desmin-related myopathy. Nat. Genet 1998; 20, 92–95.

30. Sanbe A, Yamauchi J, Miyamoto Y, Fujiwara Y, Murabe M, Tanoue A. Interruption of CryAB-Amyloid Oligomer Formation by HSP22. J Biol Chem 2007; 282: 555-63.

31. den Engelsman J, Gerrits D, de Jong WW, Robbins J, Kato K, Boelens WC. Nuclear Import of alpha B-crystallin is Phosphorylationdependent and Hampered by hyperphosphorylation of the Myopathy-related Mutant R120G J. Biol Chem 2005; 280: 37139-48.

32. Webster KA. Serine phosphorylation and suppression of apoptosis by the small heat shock protein alphaB-crystallin. Circ Res 2003; 92: 203-11.

33. Wolter KG, Hsu YT, Smith CL, Nechushtan A, Xi XG and Youle RJ. Movement of Bax from the cytosol to mitochondria during apoptosis. J. Cell Biol 1997; 139: 1281–1292.

34. Ziegler A, Nervi P, Dürrenberger M, Seelig J. The cationic cell-penetrating peptide CPP(TAT) derived from the HIV-1 protein TAT is rapidly transported into living fibroblasts: optical, biophysical, and

metabolic evidence. Biochemistry 2005; 44: 138-148.

35. Ciechanover A. The ubiquitin-proteasome pathway :on protein death and cell life. EMBO J 1998; 17: 7151–7160.

36. Lindenboim L, Yuan J and Stein R (2000) Bcl-xS and Bax induce different apoptotic pathways in PC12 cells. Oncogene 19: 1783–1793

37. Bullard KM, Lund L, Mudgett JS, Mellin TN, Hunt TK, Murphy B, Ronan J, Werb Z, Banda MJ. Impaired wound contraction in stromelysin-1-deficient mice. Ann Surg 1999; 230:260-5.

38. Dunsmore SE, Saarialho-Kere UK, Roby JD, Wilson CL, Matrisian LM, Welgus HG, Parks WC. Matrilysin expression and function in airway epithelium. J Clin Invest 1998; 102:1321-31.

39. Parcellier A, Schmitt E, Brunet M, Hammann A, Solary E, Garrido C .Small heat shock proteins HSP27 and alphaB-crystallin: cytoprotective and oncogenic functions. Antioxid Redox Signal 2005; 7: 404-13

40. Li DW, Liu JP, Mao YW, Xiang H, Wang J, Ma WY, Dong Z, Pike HM, Brown RE, Reed JC. Calcium-activated RAF/MEK/ERK signaling pathway mediates p53-dependent apoptosis and is abrogated by alpha B-crystallin through inhibition of RAS activation. Mol Biol Cell 2005; 16: 4437-53.

41. Liu JP, Schlosser R, Ma WY, Dong Z, Feng H, Liu L, Huang XQ, Liu Y, Li DW. Human alphaA- and alphaB-crystallins prevent UVA-induced apoptosis through regulation of PKC alpha, RAF/MEK/ERK and AKT signaling pathways. Exp Eye Res 2004; 79:393-403.

42. Reunanen N, Li SP, Ahonen M, Foschi M, Han J, Kahari VM. Activation of p38 alpha MAPK enhances collagenase-1 (matrix metalloproteinase (MMP)-1)and stromelysin-1 (MMP-3) expression by mRNA stabilization. J Biol Chem 2002; 277:32360–8.

43. Madlener M, Parks WC, Werner S. Matrix metalloproteinases (MMPs) and their physiological inhibitors (TIMPs) are differentially expressed during excisional skin wound repair. Exp Cell Res 1998; 242: 201–2

44. Sugioka R, Shimizu S, Funatsu T, Tamagawa H, Sawa Y, Kawakami T, et al. BH4-domain peptide from Bcl-xL exerts anti-apoptotic activity *in vivo*. Oncogene 2003; 22: 8432-40.

45. Gustafsson AB, Sayen MR, Williams SD, Crow MT, Gottlieb RA. TAT protein transduction into isolated perfused hearts: TAT-apoptosis repressor with caspase recruitment domain is cardioprotective. Circulation 2002; 106: 735-9.

46. Brooks H, Lebleu B, Vives E. Tat peptide-mediated cellular delivery: back to basics. Adv Drug Deliv Rev 2005; 57: 559-577.

47. Fittipaldi A, Giacca M. Transcellular protein transduction using the Tat protein of HIV-1. Adv Drug Deliv Rev 2005; 57: 597-608.

48. Singh BN, Rao KS, Ramakrishna T, Rangaraj N, Rao ChM. Association of alphaB-crystallin, a small heat shock protein, with actin: role in modulating actin filament dynamics in vivo. J Mol Biol 2007; 366: 756-67.

49. Ghosh JG, Houck SA, Clark JI. Interactive sequences in the stress protein

and molecular chaperone human alphaB crystallin recognize and modulate the assembly of filaments. Int J Biochem Cell Biol 2007; 39: 1804-15.

50. Ghosh JG, Estrada MR, Clark JI. Interactive domains for chaperone activity in the small heat shock protein, human alphaB crystallin. Biochemistry 2005; 44: 14854-69.

ABSTRACT (KOREAN)

AlphaB-crystallin 단백질 전달에 의한 심근보호 기능 및 기전 규명

<지도교수 장 양 수>

연세대학교 대학원 노화과학협동과정

양 승 원

작은 사이즈의 열충격 단백질 (small heat shock protein)들은 다양한 세포 내외부의 세포사멸을 초래하는 자극에 대한 세포 보호 기전이 뛰어난 것으로 알려져 있다. 그 중의 하나인 알파비 크리스탈린은 심장, 골격근, 신장과 같은 조직에 상당한 양으로 분포되어 있

으며, 세포 내 손상단백질의 회복과 세포 사멸을 억제하고 보호하는 데 중요한 단백질이다. 최근 연구들에 따르면, 다양한 세포 사멸을 유도하는 자극에서 유전자 전달 방법을 이용한 알파비 크리스탈린의 일시적인 과발현으로 세포 사멸이 상당히 억제되는 보고들이 있다. 본 연구에서는 생체 물질 전달 시스템중의 하나인 단백질 전달 도메인 (protein transduction domain, PTD)을 이용하여 알바피 크리스탈린을 심근세포로 전달하여 그 효능을 관찰하였다. 사람의 알파비 크리스탈린 cDNA을 얻은 후 단백질 전달 도메인 TAT-PTD에 융합하여 세포 내로 침투가 가능한 재조합 단백질 TAT-알파비 크리스탈린을 제조하여 본 실험에 사용하였다. 본 연구를 통해서 세포 내로 전달된 알파비 크리스탈린의 양이 높을수록 세포사멸(apoptosis) 억제 효과가 상당히 증가 되는 것을 확인 하였다. 또한 과량의 단백질이 세포 내로 전달된 경우 특정한 부분이 절단 되고, 불활성화 되는 특이한 현상을 관찰하였고, 다양한 실험을 통해서 이러한 현상에 중요하게 관여하고 있는 것이 matrix metalloproteinases (MMP)라는 것을 새롭게 규명하였다. 단백질 전달 치료 방법은 부작용이 적고 원하는 target 에 매우 직접적으로 작용 할 수 있으며, 단 시간 내에 빠른 효과를 기대 할 수 있는 장점이 있는 반면, 단백질에 특성상 세포 내에서 장시간 동안 유지 할 수 없어 오랜 효과를 기대 할 수 없는 단점을 가지고 있다. 이 연구

를 통해 단백질 전달 기술을 이용한 알파비 크리스탈린의 세포보호 효과를 확인함으로써 새로운 단백질 약물 개발 가능성을 제시해 주었으며, 세포 내로 도입된 단백질의 활성에 MMP들이 조절 작용을 한다는 것을 새롭게 확인함으로써 세포 내로 전달된 단백질의 안정성과 활성을 조절할 수 있는 가능성을 제시 하였다.

핵심 되는 말: 알파비 크리스탈린, 단백질 전달 도메인, Matrix Metalloproteinases, 열충격 단백질, 세포 사멸